

NJC

Accepted Manuscript



This is an *Accepted Manuscript*, which has been through the Royal Society of Chemistry peer review process and has been accepted for publication.

Accepted Manuscripts are published online shortly after acceptance, before technical editing, formatting and proof reading. Using this free service, authors can make their results available to the community, in citable form, before we publish the edited article. We will replace this *Accepted Manuscript* with the edited and formatted *Advance Article* as soon as it is available.

You can find more information about *Accepted Manuscripts* in the [Information for Authors](#).

Please note that technical editing may introduce minor changes to the text and/or graphics, which may alter content. The journal's standard [Terms & Conditions](#) and the [Ethical guidelines](#) still apply. In no event shall the Royal Society of Chemistry be held responsible for any errors or omissions in this *Accepted Manuscript* or any consequences arising from the use of any information it contains.

Synthesis and photoelectric properties of a solution-processable yellow-emitting Iridium (III) complex

Yuling Wu,^{ab} Huixia Xu,^{ab} Junli Yang,^{ab} Jie Li,^{ab} Wenqing Liang,^{ab} Jing Sun,^{ab}

Hua Wang,^{ab} Bingshe Xu,^{*ab}

^a Key Laboratory of Interface Science and Engineering in Advanced Materials, Taiyuan University of Technology, Taiyuan, 030024, China.

^b Research Center of Advanced Materials Science and Technology, Taiyuan University of Technology, Taiyuan, 030024, China.

Abstract: A solution-processable yellow-light-emitting heteroleptic phosphorescent Ir(III) complex of (CzhBTZ)₂Ir(fpptz)[CzhBTZ: (2-[2-(6-(9-carbazolyl)hexyl)phenyl]benzothiazole) fpptz : (2-(5-(4-fluorophenyl)-2H-1,2,4-triazol-3-yl)] were synthesized. Its photophysical, thermal and electroluminescent properties were investigated. The phosphorescent organic light-emitting diodes (PhOLEDs) using (CzhBTZ)₂Ir(fpptz) doping in (4,4'-Bis(N-carbazolyl)-1,1'-biphenyl) as the emitting layer was prepared by spin-coating with maximum peak at 533 nm, and International Commission on Illumination (CIE) coordinates of (0.42, 0.56), respectively.

Key word: Solution-processable; Iridium(III) complex; Electroluminescent properties; Spin-coating; Yellow-light-emitting

1. Introduction

In recent years, much research interest has been focused on the organic light-emitting devices (OLEDs) which can be applied in full color display and prospective illumination¹⁻⁴. The phosphorescent complexes can realize theoretical 100% internal quantum efficiency due to the ability to harvest both singlet and triplet excitons⁵⁻⁷. Therefore, synthesis of high performance phosphorescent materials is one of the effective ways to improve the efficiency of OLED. The performances of Iridium(III) complexes are better⁸ than the others due to their high efficiencies and facile color tunabilities^{9,10}.

The yellow Iridium(III) complexes play an important role for realizing full-color display as well as high-performance two-color (blue and yellow) white OLEDs^{11,12}. Moreover, it exhibit superiority in both efficiency and fabrication cost compared with

three-color (blue, green and red) analogues as solid-state lighting sources, and thus the development of highly efficient yellow heavy metal complexes is a pressing concern¹³⁻¹⁵.

Therefore, the solution-processable^{16, 17} phosphorescent Ir(III) complex of (CzhBTZ)₂Ir(fpptz) has been designed and synthesized. The introduction of hexyl chain in main ligand could increase steric-hindrance effect, weaken intermolecular stack, effectively improve the solubility of compounds, prevent the interaction of triplet excitons, reduce the non-radiative transition and eventually improve the luminous efficiency¹⁸. Carbazole^{19, 20} (Cz) and 1, 2, 4-triazol^{9, 21} were introduced in Ir(III) complexes because of their unique hole and electron-transporting properties. Consequently, the carrier-transport balance will be improved in PhOLEDs²². Besides, the auxiliary ligand is N, N'-aromatic heterocyclic ligand, which has higher triplet energy level as the strong field ligand, and the lone pair electrons of N atom contained in the ligand can adjust the LUMO energy levels of complexes⁹. In this article, the thermal, photoluminescent (PL), film-forming and EL properties of the synthesized complexes were further investigated.

2. Experimental section

2.1 General information

All chemicals and reagents were used as received from commercial sources without further purification. Solvents for chemical synthesis were purified according to the standard procedures. Thereinto, 2-Ethoxyethanol, 2-Cyanopyridine, 2-Fluorobenzoyl chloride, salicylic acid and 2-Aminothiophenol were purchased from J&K chemical technology company, 1,6-Dibromohexane and Carbazole were purchased from Energy Chemical technology company. Other reagents were commercially available analytical pure.

¹H NMR spectra were measured on a Bruker DRX 600 spectrometer, and chemical shifts were reported in ppm using tetramethylsilane (TMS) as an internal standard. The UV-visible absorption spectra were determined on a Hatachi U-3900 spectrophotometer and the photoluminescence (PL) emission spectra were obtained using a Horiba FluoroMax-4 spectrophotometer at room temperature in the CHCl₃

solution with concentration of 1.0×10^{-5} mol/L. Thermogravimetric analysis (TGA) was recorded on a French Setaram thermogravimetry at a heating rate of $10^\circ\text{C}/\text{min}$ with the gas flow rate of $30 \text{ ml}/\text{m}^3$ under nitrogen atmosphere. Atomic force microscopy (AFM) measurements were performed on a SPA-300HV from Digital Instruments Inc. (Santa Barbara, CA) in the tapping mode. Cyclic voltammetry (CV) data were undertaken with Autolab/PG STAT302 electrochemical workstation at the scanning rate of $20 \text{ mV}/\text{s}$ at room temperature under the protection of nitrogen using platinum (Pt) filament as working electrode, Pt plate as the counter electrode, and a saturated calomel electrode as the reference electrode. Tetrabutyl ammonium perchlorate (TBAP, 0.1M) solution as the supporting electrolyte and $(\text{CzhBTZ})_2\text{Ir}(\text{fpptz})$ were dissolved in acetonitrile (CH_3CN).

2.2 Device Fabrication and Characterization.

Patterned glass substrates coated with indium tin oxide (ITO) ($20 \Omega \text{ square}^{-1}$) were cleaned by a surfactant scrub, washed successively with deionized water, acetone and isopropanol in an ultrasonic bath, and then dried at 120°C for 8 h. A 40-nm-thick poly(3,4-ethylenedioxythiophene) : poly(styrenesulfonic acid) (PEDOT:PSS) as hole-injection layer was spin-coated on top of ITO and baked in a vacuum at 120°C for 20 min. Thin film (50 nm thick) of the $(\text{CzhBTZ})_2\text{Ir}(\text{fpptz})$ as the emitting guest and (4,4'-Bis(N-carbazolyl)-1,1'-biphenyl) CBP as the host was deposited on top of the PEDOT:PSS layer by spin-coating in chlorobenzene solution, followed by thermal annealing at 110°C for 20 min. Then an electron-transporting layer of 1,3,5-tris(N-phenylbenzimidazol-2-yl)benzene (TPBI, 35 nm) and LiF (1 nm) / Al (150 nm) as the cathode were deposited by vacuum evaporation under a base pressure of 5×10^{-4} Pa. The emission areas of the devices were 6 mm^2 .

The electroluminescence (EL) spectra were measured with a PR655 spectrascan spectrometer. The current-voltage-luminance characteristics and CIE coordinates were measured with a Keithley 2400 programmable voltage current source. The luminance of the device was measured with a Hitachi F-4600 fluorescence spectrophotometer.

2.3 Synthesis of ligands and complexes

Synthetic routes of ligands and complexes are displayed in Scheme.1

2.3.1 9-(6-bromine hexyl)carbazole (BrhCz)²³⁻²⁵ (1)

The mixture of carbazole (30 mmol), 1,6-dibromo hexane (90 mmol) and adequacy

tetrabutyl ammonium bromide (TBAB) in 50 mL toluene was stirred uniform and then added potassium hydroxide solution (16 mol/L) and heat to reflux for 12 h under nitrogen atmosphere. After cooled to room temperature, the mixture was extracted with water and methylene chloride (CH_2Cl_2), dried by anhydrous magnesium sulfate and then concentrated by rotary evaporation. Finally, it was purified by column chromatography on silica gel with petroleum ether: $\text{CH}_2\text{Cl}_2 = 20:1$ as eluent to obtain the white acicular crystal. Yield: 87%. ^1H NMR (CDCl_3) δ : 8.11 (d, $J = 7.8$ Hz, 2H), 7.47 (ddd, $J_1 = 1.2$ Hz, $J_2 = 7.2$ Hz, $J_3 = 8.4$ Hz, 2H), 7.41 (d, $J = 7.8$ Hz, 2H), 7.24 (ddd, $J_1 = 1.2$ Hz, $J_2 = 7.2$ Hz, $J_3 = 7.8$ Hz, 2H), 4.32 (t, $J = 7.2$ Hz, 2H), 3.37 (t, $J = 6.6$ Hz, 2H), 1.93-1.88 (m, 2H), 1.84-1.79 (m, 2H), 1.50-1.45 (m, 2H), 1.43-1.38 (m, 2H). HR-MS: Calcd.329.0799; Found 329.0803.

2.3.2 2-(2-hydroxyphenyl)benzothiazole (BTZH) (2)

The mixture of salicylic acid (30 mmol), 2-aminothiophenol (36 mmol) and toluene (120 mL) was heated to 80 °C for 1 h. After cooling to 40 °C, PCl_3 was added slowly and then was heated to reflux for 6 h. Finally, the solvent was cooled to room temperature to separate out the white solid. The white acicular crystals BTZH were obtained. Yield: 92%. ^1H NMR (CDCl_3) δ : 12.79 (s, 1H), 8.78 (d, $J = 4.8$ Hz, 1H), 8.35 (t, $J_1 = J_2 = 9.6$ Hz, 3H), 7.93 (dt, $J_1 = 1.8$ Hz, $J_2 = 7.8$ Hz, 1H), 7.74 (d, $J = 8.4$ Hz, 2H), 7.46 (ddd, $J_1 = 1.2$ Hz, $J_2 = 4.8$ Hz, $J_3 = 7.8$ Hz, 1H). HR-MS: Calcd.227.0405; Found 227.0409.

2.3.3 2-[2-(6-(9-carbazolyl)hexyl)phenyl]benzothiazole (CzhBTZ) (3)

Under nitrogen atmosphere, the mixture of BrCz (4 mmol), BTZH (5mmol) and DMF (30 mL) was stirred uniform and then of potassium carbonate solution (2 mol/L) was added and appropriate potassium iodide to react for 30 min at room temperature. The reaction solution was poured into ice water to separate out white precipitation after it was heated to reflux for 24 h, which was filtered, dried and recrystallized by CH_2Cl_2 to obtain white solid, yield 72%. ^1H NMR (CDCl_3) δ : 8.54 (dd, $J_1 = 1.8$ Hz, $J_2 = 7.8$ Hz, 1H), 8.11 (dt, $J_1 = 1.2$ Hz, $J_2 = 7.8$ Hz, 2H), 8.08 (dt, $J_1 = 0.6$ Hz, $J_2 = 8.4$

Hz, 1H), 7.82 (d, $J = 7.8$ Hz, 1H), 7.47 (d, $J = 8.4$ Hz, 1H), 7.45 (dd, $J_1 = 1.2$ Hz, $J_2 = 7.2$ Hz, 2H), 7.43-7.41 (m, 3H), 7.35 (ddd, $J_1 = 1.2$ Hz, $J_2 = 7.2$ Hz, $J_3 = 7.8$ Hz, 1H), 7.24 (ddd, $J_1 = 1.2$ Hz, $J_2 = 6.6$ Hz, $J_3 = 7.8$ Hz, 2H), 7.20 (ddd, $J_1 = 1.2$ Hz, $J_2 = 7.8$ Hz, $J_3 = 8.4$ Hz, 1H), 7.00 (d, $J = 8.4$ Hz, 1H), 4.34 (t, $J = 7.2$ Hz, 2H), 4.16 (t, $J = 6.6$ Hz, 2H), 2.01-1.94 (m, 4H), 1.69-1.64 (m, 2H), 1.55-1.50 (m, 2H). HR-MS: Calcd.476.1922; Found 476.1926.

2.3.4 2-(5-(4-fluorinated phenyl)-1,3,4-triazole)pyridine (fpptz) (4)

Under nitrogen atmosphere, the mixture of 2-cyanopyridine (50 mmol), hydrazine hydrate (50 mmol) and ethanol (25 mL) was reacted for 8 h at low temperature to produce viscous light yellow paste and cooled to room temperature. The redundant ethanol was removed in vacuum. The obtained solid was washed by a small quantity of diethyl ether, suction filtered and dried for 3 h to obtain white crystal (2-pyridine)amidrazone.

Under nitrogen atmosphere, the mixture of (2- pyridine)amidrazone (30 mmol), Na_2CO_3 (30 mmol), 2-Fluorobenzoyl chloride (30 mmol) and THF (30 mL) were reacted for 6 h and filter. The filter mass was heated to elevated temperature for 30 min in 30 ml ethylene glycol to dehydrate, dried for 8 h under vacuum. Then it was recrystallized by ethanol to obtain the white acicular crystal. Yield 92%. ^1H NMR (DMSO- d_6) δ : 14.87 (s, 1H), 8.74 (d, $J = 4.8$ Hz, 1H), 8.18 (d, $J = 7.8$ Hz, 1H), 8.15-8.11 (d, $J = 7.8$ Hz, 2H), 8.04 (dt, $J_1 = 1.2$ Hz, $J_2 = 7.2$ Hz, 1H), 7.57 (ddd, $J_1 = 0.6$ Hz, $J_2 = 4.8$ Hz, $J_3 = 5.4$ Hz, 1H), 7.34 (t, $J = 9.0$ Hz, 2H). HR-MS: Calcd.240.0811; Found 240.0815.

2.3.5 2-[2-(6-(9- carbazoly)l hexyl) phenyl] benzothiazole chloro-bridge iridium dimers [(CzhBTZ) $_2$ Ir(μ -Cl) $_2$ Ir(CzhBTZ) $_2$] (5)

The mixture trihydrate trichloride iridium ($\text{IrCl}_3 \cdot 3\text{H}_2\text{O}$) (0.1 mmol) in 2-ethoxyethanol (24 mL) and deionized water (8 mL) and 2-[2-(6-(9- carbazoly)l hexyl) phenyl] benzothiazole (0.25 mmol) was heated to reflux for 24 h under nitrogen atmosphere. After cooling to room temperature, the deionized water (200 mL)

was poured into the reaction solution to separate out atrovirens flocculent solid, filtered and washed with deionized water and ethanol. The crude product was dried for 12 h at 45 °C under vacuum to obtain the green solid.

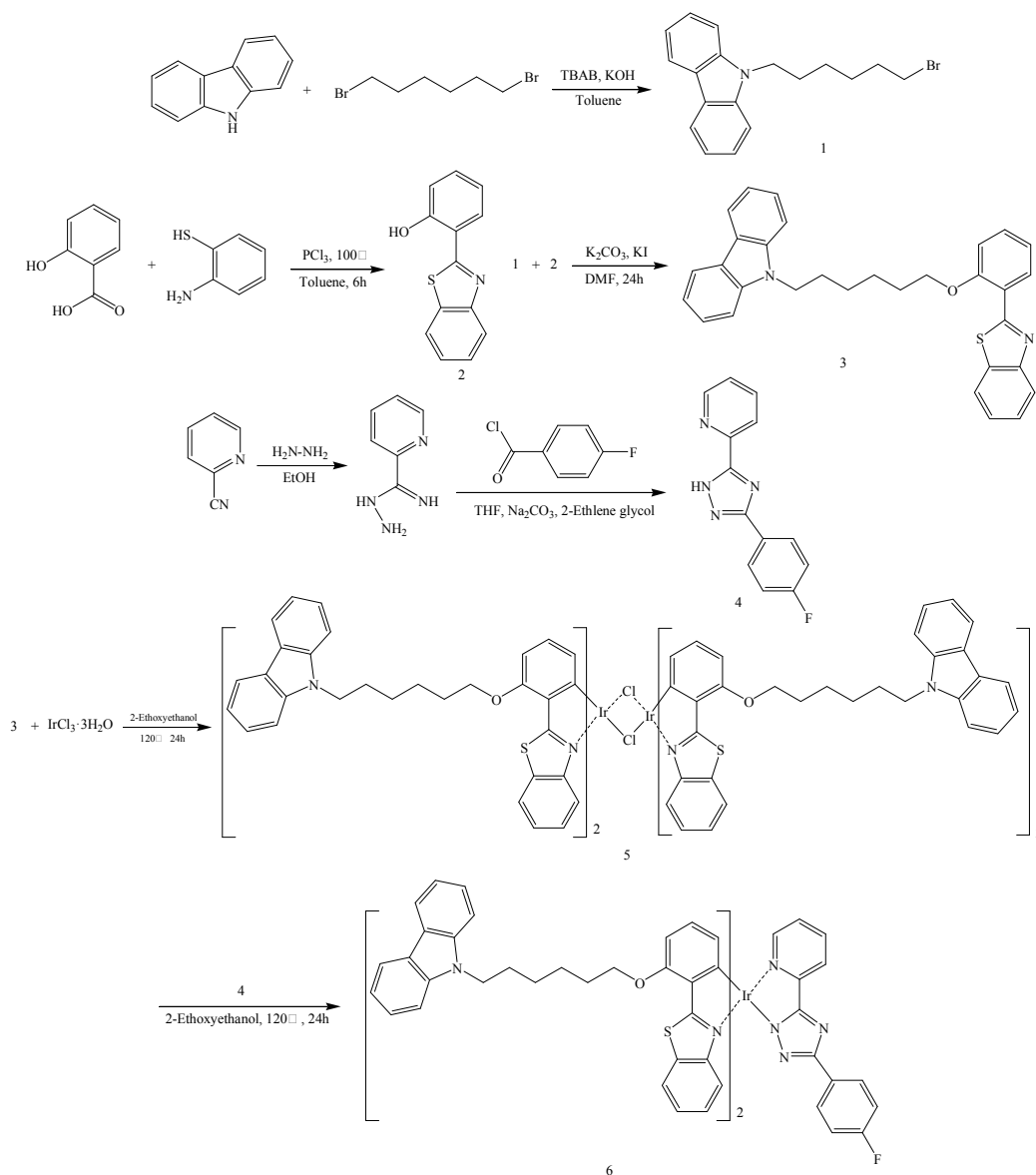
2.3.6 (CzhBTZ)₂Ir(fpptz) (6)

The solution of the chloro-bridged iridium (0.1 mmol) in 2-ethoxyethanol (25 mL), the 2-(5-(4-fluorinated phenyl)-1,3,4-triazole)pyridine (0.25 mmol) and anhydrous potassium carbonate (2.0 mmol) were stirred at 100 °C for 24 h under nitrogen atmosphere. After cooling to room temperature, Deionized water was added to separate out green flocculent solid, and then purified by column chromatography on silica gel with petroleum ether : CH₂Cl₂ = 10:1 as eluent to obtain the yellow solid powder. Yield: 70%. ¹H NMR (CDCl₃) δ: 8.17 (d, *J* = 7.8 Hz, 1H), 8.10 (t, *J* = 8.4 Hz, 6H), 7.84 (d, *J* = 4.8 Hz, 1H), 7.75 (t, *J* = 7.8 Hz, 1H), 7.64 (dd, *J*₁ = 8.4 Hz, *J*₂ = 11.4 Hz, 2H), 7.45-7.40 (m, 8H), 7.24-7.18 (m, 5H), 7.09 (t, *J* = 7.2 Hz, 1H), 7.05 (t, *J* = 6.6 Hz, 1H), 6.99 (t, *J* = 9.0 Hz, 2H), 6.91-6.89 (m, 2H), 6.77-6.72 (m, 2H), 6.42 (dd, *J*₁ = 4.2 Hz, *J*₂ = 8.4 Hz, 2H), 6.22 (d, *J* = 9.0 Hz, 1H), 6.02 (dd, *J*₁ = 7.2 Hz, *J*₂ = 15 Hz, 2H), 4.36 (t, *J* = 7.2 Hz, 2H), 4.33 (t, *J* = 7.2 Hz, 2H), 4.18-4.07 (m, 4H), 2.01-1.95 (m, 8H), 1.71-1.66 (m, 4H), 1.57-1.52 (m, 4H). HR-MS: Calcd.907.2206; Found 907.2209.

3. Results and discussion

3.1 Synthesis and characterization

Scheme 1 displays our synthetic route towards (CzhBTZ)₂Ir(fpptz). We synthesized the phenylbenzothiazole derivative (2-[2-(6-(9-carbazolyl)hexyl)phenyl]benzothiazole) (3) with introducing the N-hexyl carbazole (1), which could improve the hole transporting ability and (2-(5-(4-fluorophenyl)-2H-1,2,4-triazol-3-yl) gave (CzhBTZ)₂Ir(fpptz) in 70% yield.

Scheme.1. Synthesis of $(\text{CzhBTZ})_2\text{Ir}(\text{fpptz})$

3.2 Photophysical properties

Figure 1 shows the UV-visible absorption and photoluminescence (PL) emission spectra of $(\text{CzhBTZ})_2\text{Ir}(\text{fpptz})$ in CHCl_3 solution and in neat films. The phosphorescence spectrum was measured in 2-methyltetrahydrofuran at 77 K. There are two intense absorption peaks seated at 239 and 265 nm and a moderate one seated at 295 nm, which are attributed to the spin-allowed ligand-centered (^1LC) transitions. The weak absorption peaks at 332 and 345 nm were assigned to the spin-allowed metal-to-ligand charge-transfer ($^1\text{MLCT}$) transitions²⁶. The weaker absorption peak located at 432 nm due to the spin-inhibited metal-to-ligand charge-transfer ($^3\text{MLCT}$)

state mixed with ligand-centered (^3LC) transitions²⁷. In films, the complex exhibits the similar UV-vis absorption pattern with that of in solution, but the absorption peaks at 228 and 264 nm appear blue shift due to the different aggregative state.

The emission peaks of $(\text{CzhBTZ})_2\text{Ir}(\text{fpptz})$ in dilute solution located at 528 nm (excitation wavelength of 365 nm) and a shoulder at 561 nm are attributed to the metal-to-ligand charge-transfer ($^3\text{MLCT}$) state transitions^{28, 29}. The maximum emission bands of the complex in neat films, centered at 533 nm and with a shoulder at 570 nm, is similar to that provided by its solution, implying that no significant intermolecular interactions occur in the ground state. At 77 K, the maximum emission peak of $(\text{CzhBTZ})_2\text{Ir}(\text{fpptz})$ is 532 nm and with the shoulder peak at 569 nm under the excitation wavelength of 365 nm without exquisite structure vibration, which indicate the dominant phosphorescence emission state of the complex should be metal-to-ligand charge-transfer ($^3\text{MLCT}$) state transitions^{30, 31}. Thus, it is inferred that the triplet energy level (E_T) of $(\text{CzhBTZ})_2\text{Ir}(\text{fpptz})$ is 2.33 eV.

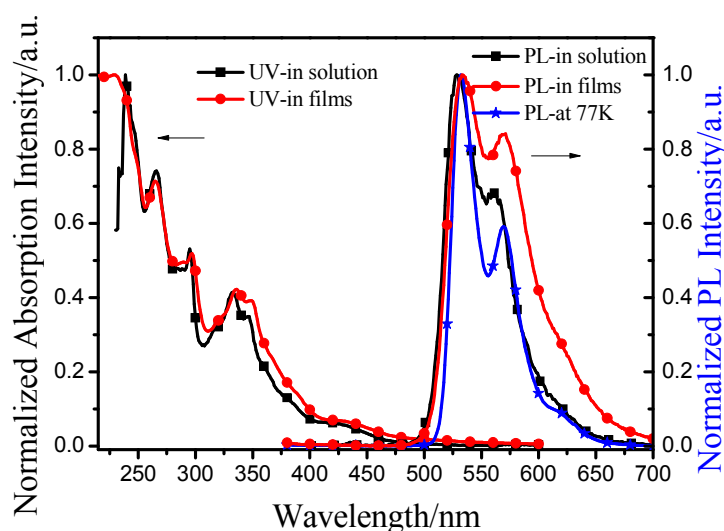


Fig.1. UV-visible absorption and emission spectra of $(\text{CzhBTZ})_2\text{Ir}(\text{fpptz})$ in CHCl_3 solution of at a concentration of 1.0×10^{-5} mol / L at 298 K and in neat films and phosphorescence spectrum in 2-methyltetrahydrofuran at 77 K.

According to the computational formula Tauc^{32} , the optical band gap (E_g) of $(\text{CzhBTZ})_2\text{Ir}(\text{fpptz})$ could be calculated through the relationship between UV-visible absorption spectra and absorption coefficient.

$$\alpha h\nu = B(h\nu - E_g)^{n/2}$$

α , h , ν and E_g express respectively absorption factor, planck constant, the frequency of

light waves (Hz), and optical band gap (eV), and B is proportionality coefficient in the formula. The n of the formula show the electron transition characteristics of the material such as n = 1 corresponding to direct transition and n = 4 corresponding to indirect transition. Under normal circumstances, the transition of (CzhBTZ)₂Ir(fpptz) is direct transition^{33,34}. Hence, the curve of $(h\nu A)^2 - h\nu$ was obtained (Figure 2, n=1 at the same time α and absorbancy (A) and the band gap of (CzhBTZ)₂Ir(fpptz) was calculated to be 2.55 eV whit getting $h\nu$ by $1240/A$.

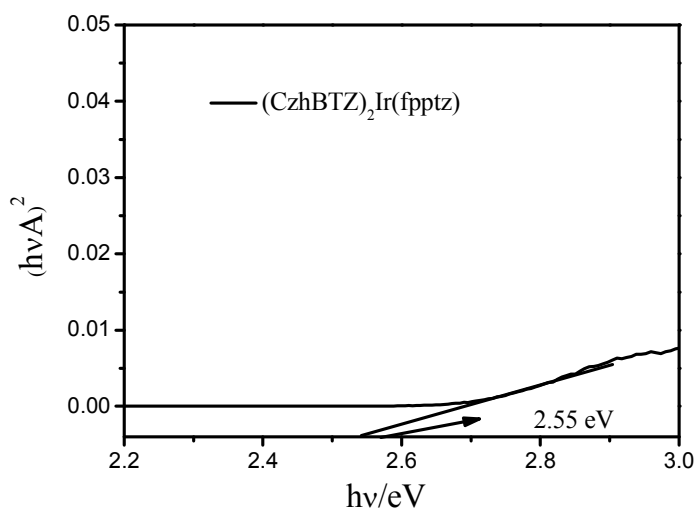


Fig.2. The $(h\nu A)^2 - h\nu$ curve of (CzhBTZ)₂Ir(fpptz)

3.3 Electrochemical properties

The cyclic voltammetry curve of (CzhBTZ)₂Ir(fpptz) in CHCl₃ solution using ferrocene as the internal standard substance is showed in Figure 3. The initial oxidation potential of the complex (E_c^{ox}) and ferrocene (E_f^{ox}) are 1.176 and 0.435 V, respectively. The energy level (relative to the vacuum level) of the highest occupied molecular orbital (E_{HOMO}) of -5.54eV were obtained by the following formula³⁵.

$$E_{HOMO} = -4.8 - e(E_c^{ox} - E_f^{ox})$$

The E_{LUMO} of (CzhBTZ)₂Ir(fpptz) is -2.99 eV by $E_{LUMO} = E_{HOMO} + E_g$ (2.55 eV).

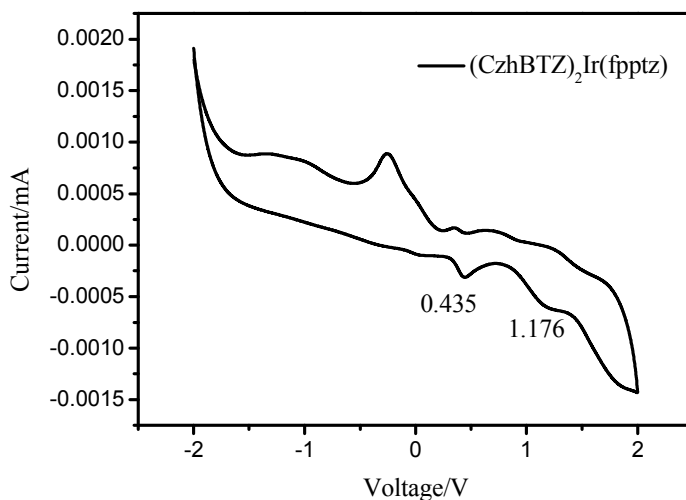


Fig.3. The cyclic voltammetry curve of (CzhBTZ)₂Ir(fpptz) in CHCl₃ solution with the concentration of 1×10^{-3} M at a scanning rate of 20 mVs^{-1} .

3.4 Thermal properties and morphological stability of thin films

Thermal stability is one of the important indices for performance evaluation of organic electroluminescent materials. Figure 4 displays the TGA curve of (CzhBTZ)₂Ir(fpptz), in which can be seen the weight loss of (CzhBTZ)₂Ir(fpptz) is only 5% when the temperature is up to $321 \text{ }^\circ\text{C}$.

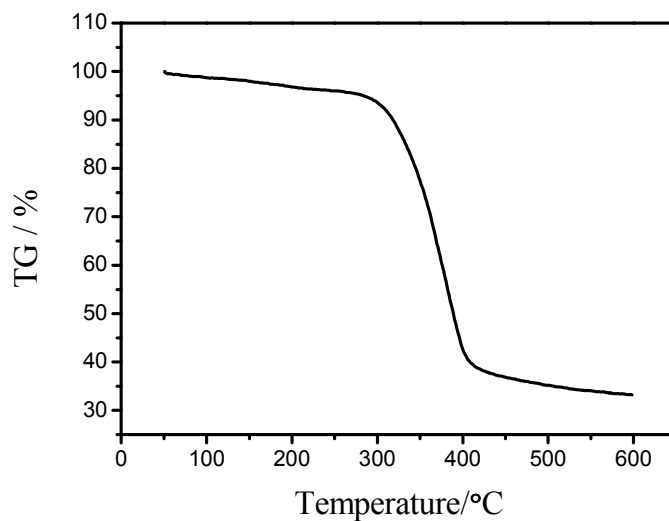


Fig.4. TGA curves of (CzhBTZ)₂Ir(fpptz) in nitrogen atmosphere with a heating rate of $10^\circ\text{C}/\text{min}$.

In order to further characterize the film-forming properties, the (CzhBTZ)₂Ir(fpptz) was dissolved in chlorobenzene with the concentration of

1.82×10^{-2} mol/L and then was spin-coated on pre-cleaned indium tin oxide (ITO) substrates. The surface morphology was characterized by use of atomic force microscopy (AFM) with scanned area being $5 \times 5 \mu\text{m}$. Figure 5 reveals the two-dimension and three-dimension images of the film. The results indicate that $(\text{CzhBTZ})_2\text{Ir}(\text{fpptz})$ possesses good film-forming ability, uniform thin film and the root-mean-square (RMS) roughness is 2.782 nm. The thickness of the formed film is 30.24 nm.

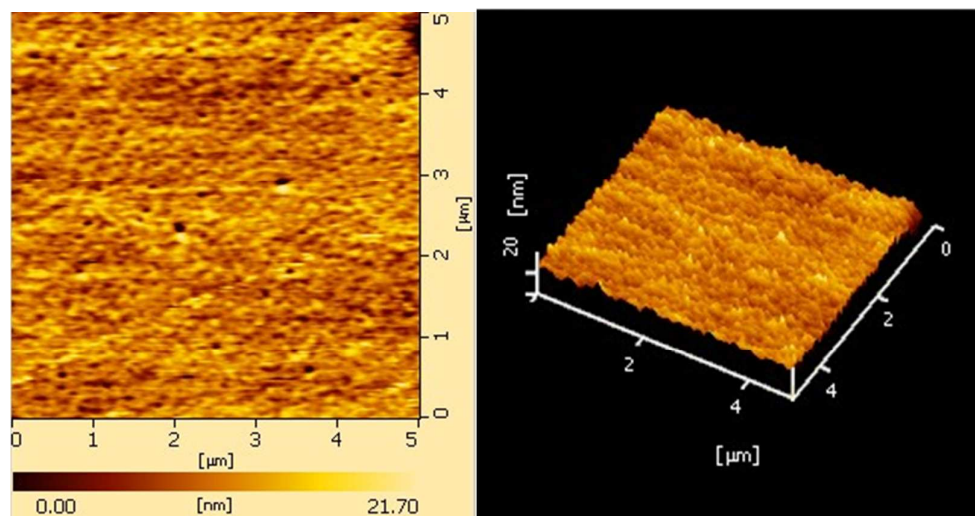


Fig.5. AFM images of spin coated $(\text{CzhBTZ})_2\text{Ir}(\text{fpptz})$ film on ITO substrate.

3.5 Electroluminescent properties

In order to characterize the electroluminescent properties of $(\text{CzhBTZ})_2\text{Ir}(\text{fpptz})$, The devices with a configuration of ITO/ PEDOT:PSS(40 nm)/ $(\text{CzhBTZ})_2\text{Ir}(\text{fpptz})$: CBP(8 wt%) (40-50nm)/ TPBi(40 nm)/ LiF(1 nm)/ Al(150 nm) were fabricated by spin-coating, which using the $(\text{CzhBTZ})_2\text{Ir}(\text{fpptz})$ as emitting guest, CBP as the host and chlorobenzene as the solvent (as shown in Figure 6), and TPBi as a hole-blocking layer.

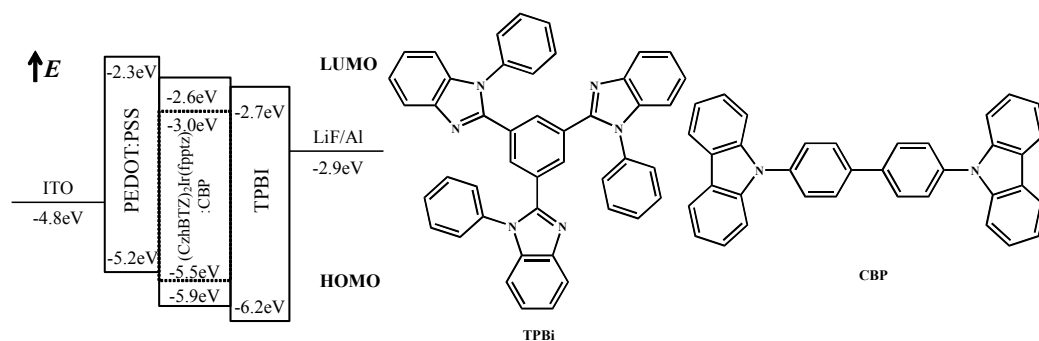


Fig.6. The device configuration and structures of the materials.

The electroluminescent peaks located at 533 and 571 nm are displayed in Figure 7, which consistent with PL spectra in neat films. Also, there is not the characteristic emission peak of CBP (λ_{\max} = 369 nm), which manifests the electroluminescence of the device derive from (CzhBTZ)₂Ir(fpptz). When voltages vary from 8 to 12 V, the luminescent intensity of shoulder peak at 571 nm slightly enhances with the increase of voltage. The color coordinates (CIE) are basically stable located at (0.42, 0.56) in the yellow-light area, which indicates that (CzhBTZ)₂Ir(fpptz) has very good spectral stability.

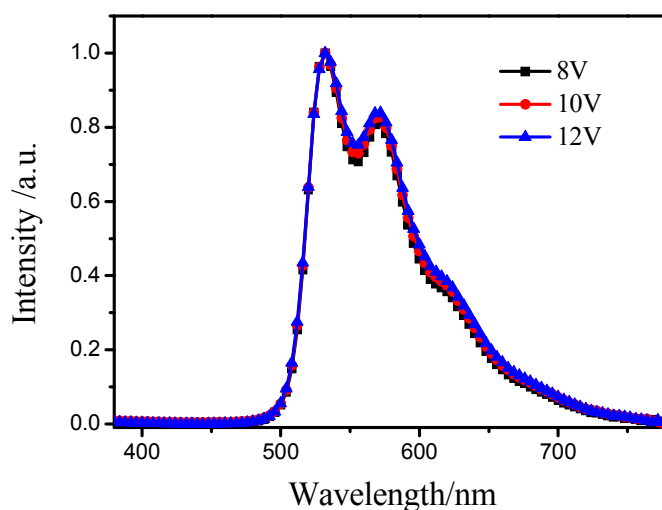


Fig.7. EL spectra under different driven voltages

The J - V - L curves of devices are shown in Figure 8. The turn-on voltage is 4.7 V and it achieves the maximum brightness 9617 cd/m² at the driving voltage of 13.8 V. From the current efficiency-current density-power efficiency (η_c - J - η_p) curves, the maximum current efficiency and the maximum power efficiency reach 9.43 cd/A and 3.29 lm/W at the current density 13.05 mA/cm², respectively. As can be seen from Figure 9, the efficiencies decrease quite slowly with increasing current density, suggesting that the introduction of N-hexyl carbazole could efficiently increase steric-hindrance effect and widen the distance between the neighboring Ir(III) complex molecules to inhibit the quenching and reduce the roll-offs phenomenon of the device. The maximum brightness is higher than that of the complex (2450 cd/m²) reported by Jin et al¹⁰. However, the turn on voltage is higher (4.7 V vs. 3.0 V) and the

maximum current efficiency is lower (9.43 vs. 10.98 cd/A) than the complex mentioned above. Hence, the device performance will be further optimized in the coming work.

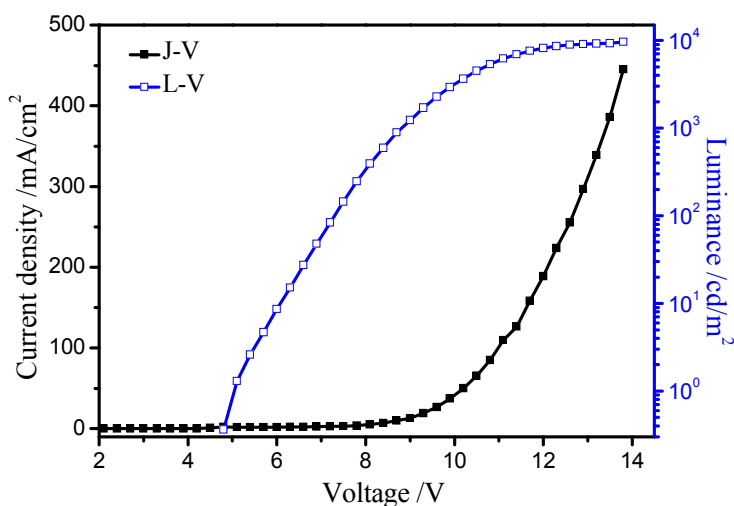


Fig.8. *J-V-L* curves of Devices.

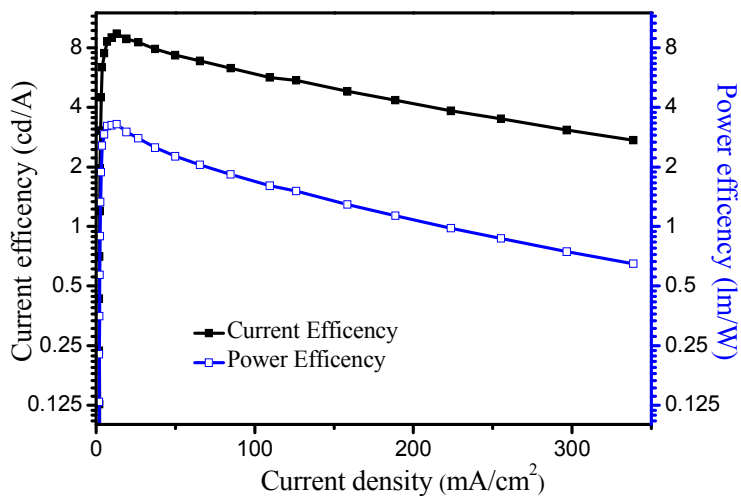


Fig.9. Current efficiency (η_c)-current density (J)-cower efficiency (η_p) curves of Devices.

4. Conclusions

In conclusion, a solution-processable heteroleptic Ir(III) complex (CzhBTZ)₂Ir(fpptz) with N-hexyl carbazole introduced into main ligand and 1, 2, 4-triazol into auxiliary ligand was designed and synthesized. The introduction of

N-hexyl carbazole could efficiently increase steric-hindrance effect to suppress the intramolecular interactions efficiently, and help to form amorphous spin-coating films. The emission bands of the (CzhBTZ)₂Ir(fpptz) showed no obvious bathochromic shifts in solid films with respect to those in dilute solution. (CzhBTZ)₂Ir(fpptz) exhibits good EL properties with a low turn-on voltage of about 4.7 V and the CIE coordinates of (0.42, 0.56). The maximum brightness, maximum current efficiency and maximum power efficiency are 9617 cd/m², 9.43 cd/A and 3.29 lm/W, respectively. The results of OLED show that (CzhBTZ)₂Ir(fpptz) is a kind of potential yellow phosphor materials (emitter) that could be applied to the flexible display in OLEDs.

Acknowledgments

This work was financially supported by the “Program for New Century Excellent Talents (NCET) in University” (NCET-13-0927), the International Science & Technology Cooperation Program of China (2012DFR50460), the National Natural Science Foundation of China (21071108, 21101111, 61274056, 61205179, 61307030, 61307029), and the Shanxi Provincial Key Innovative Research Team in Science and Technology (2012041011), Natural Science Foundation of Shanxi Province (2015021070).

References

1. D. Sun, Q. Fu, Z. Ren, W. Li, H. Li, D. Ma and S. Yan, *J. Mater. Chem. C*, 2013, **1**, 5344.
2. Q. L. Xu, H.-Y. Li, C. C. Wang, S. Zhang, T. Y. Li, Y. M. Jing, Y. X. Zheng, W. Huang, J. L. Zuo and X. Z. You, *Inorg. Chim. Acta*, 2012, **391**, 50-57.
3. Y. C. Zhu, L. Zhou, H. Y. Li, Q. L. Xu, M. Y. Teng, Y. X. Zheng, J. L. Zuo, H. J. Zhang and X. Z. You, *Adv. Mater.*, 2011, **23**, 4041-4046.
4. K. Chao, K. Shao, T. Peng, D. Zhu, Y. Wang, Y. Liu, Z. Su and M. R. Bryce, *J. Mater. Chem. C*, 2013, **1**, 6800.

5. D. Sun, Q. Fu, Z. Ren, H. Li, D. Ma and S. Yan, *Polym. Chem.*, 2014, **5**, 220-226.
6. J. X. Cai, T. L. Ye, X. F. Fan, C. M. Han, H. Xu, L. L. Wang, D. G. Ma, Y. Lin and P. F. Yan, *J. Mater. Chem.*, 2011, **21**, 15405.
7. A. Y. Tam, D. P. Tsang, M. Y. Chan, N. Zhu and V. W. Yam, *Chem. Commun. (Camb)*, 2011, **47**, 3383-3385.
8. H. Tang, L. Wei, J. Wang, Y. Li, H. Wu, W. Yang and Y. Cao, *Synth. Met.*, 2014, **187**, 209-216.
9. Enrico Orselli, Gregg S. Kottas, Asgeir E. Konradsson, Paolo Coppo, Roland Frohlich, Luisa De Cola, Addy van Dijken, Michael Bulchel and H. Bolrner, *Inorg. Chem.*, 2007, **46**, 11082-11093.
10. T. Giridhar, W. Cho, J. Park, J. S. Park, Y. S. Gal, S. Kang, J. Y. Lee and S. H. Jin, *J. Mater. Chem. C*, 2013, **1**, 2368.
11. C. Fan and C. Yang, *Chem. Soc. Rev.*, 2014, **43**, 6439-6469.
12. C. L. Ho and W. Y. Wong, *Molecular Design and Applications of Photofunctional Polymers and Materials*, 2012, 1-30.
13. X. Ouyang, D. Chen, S. Zeng, X. Zhang, S. Su and Z. Ge, *J. Mater. Chem.*, 2012, **22**, 23005.
14. B. Liang, Y. Xu, Z. Chen, J. Peng and Y. Cao, *Synth. Met.*, 2009, **159**, 1876-1879.
15. C. Sahin, I. Oner and C. Varlikli, *RSC Adv.*, 2014, **4**, 46831-46839.
16. L. Duan, L. Hou, T. W. Lee, J. Qiao, D. Zhang, G. Dong, L. Wang and Y. Qiu, *J. Mater. Chem.*, 2010, **20**, 6392.
17. T. Earmme and S. A. Jenekhe, *J. Mater. Chem.*, 2012, **22**, 4660.
18. L. Chen, Z. Ma, J. Ding, L. Wang, X. Jing and F. Wang, *Chem. Commun. (Camb)*, 2011, **47**, 9519-9521.
19. H. Xu, D. H. Yu, L. L. Liu, P. F. Yan, L. W. Jia, G. M. Li and Z. Y. Yue, *J. Phys. Chem. B*, 2010, **114**, 141-150.
20. W. C. Lin, W. C. Huang, M. H. Huang, C. C. Fan, H. W. Lin, L. Y. Chen, Y. W. Liu, J. S. Lin, T. C. Chao and M. R. Tseng, *J. Mater. Chem. C*, 2013, **1**, 6835.

21. W. Y. Hung, G. M. Tu, S. W. Chen and Y. Chi, *J. Mater. Chem.*, 2012, **22**, 5410.
22. J. Zhuang, W. Li, W. Su, M. Zhou and Z. Cui, *New J. Chem.*, 2014, **38**, 650-656.
23. L. Chen, Z. Ma, J. Ding, L. Wang, X. Jing and F. Wang, *Org. Electron.*, 2012, **13**, 2160-2166.
24. Y. Deng, S. J. Liu, Q. L. Fan, C. Fang, R. Zhu, K. Y. Pu, L. H. Yuwen, L. H. Wang and W. Huang, *Synth. Met.*, 2007, **157**, 813-822.
25. K. Yabuuchi, Y. Tochigi, N. Mizoshita, K. Hanabusa and T. Kato, *Tetrahedron*, 2007, **63**, 7358-7365.
26. B. Du, L. Wang, H. Wu, W. Yang, Y. Zhang, R. Liu, M. Sun, J. Peng and Y. Cao, *Chemistry*, 2007, **13**, 7432-7442.
27. Q. Zhao, C. Y. Jiang, M. Shi, F. Y. Li, T. Yi, Y. Cao and C. H. Huang, *Organometallics*, 2006, **25**, 3631-3638.
28. R. Ragni, E. A. Plummer, K. Brunner, J. W. Hofstraat, F. Babudri, G. M. Farinola, F. Naso and L. De Cola, *J. Mater. Chem.*, 2006, **16**, 1161.
29. S. J. Lee, J. S. Park, M. Song, I. A. Shin, Y. I. Kim, J. W. Lee, J. W. Kang, Y. S. Gal, S. Kang, J. Y. Lee, S. H. Jung, H. S. Kim, M. Y. Chae and S. H. Jin, *Adv. Funct. Mater.*, 2009, **19**, 2205-2212.
30. H. C. Ting, Y. M. Chen, H. W. You, W. Y. Hung, S. H. Lin, A. Chaskar, S. H. Chou, Y. Chi, R. H. Liu and K. T. Wong, *J. Mater. Chem.*, 2012, **22**, 8399.
31. M. Zhu, T. Ye, X. He, X. Cao, C. Zhong, D. Ma, J. Qin and C. Yang, *J. Mater. Chem.*, 2011, **21**, 9326.
32. L. Jiao, I. Chen, R. W. Collins, C. R. Wronski and N. Hata, *Applied Physics Letters*, 1998, **72**, 1057-1059.
33. N. F. Mott, R. W. Gurney, *Electronic Processes in Ionic Crystals*, Oxford Univ. Press, London, 1940.
34. Y. Y. Hao, J. Li, Z. X. Gao, H. Wang, H. F. Zhou, X. G. Liu and B. S. Xu, *Chin. J. Lumin.*, **2006**, **27**(2):254-258
35. H. X. Xu, B. S. Xu, X. H. Fang, L. Q. Chen, H. Wang and Y. Y. Hao, *J.*

Photochem. Photobiol. A: Chem., 2011, **217**, 108-116.

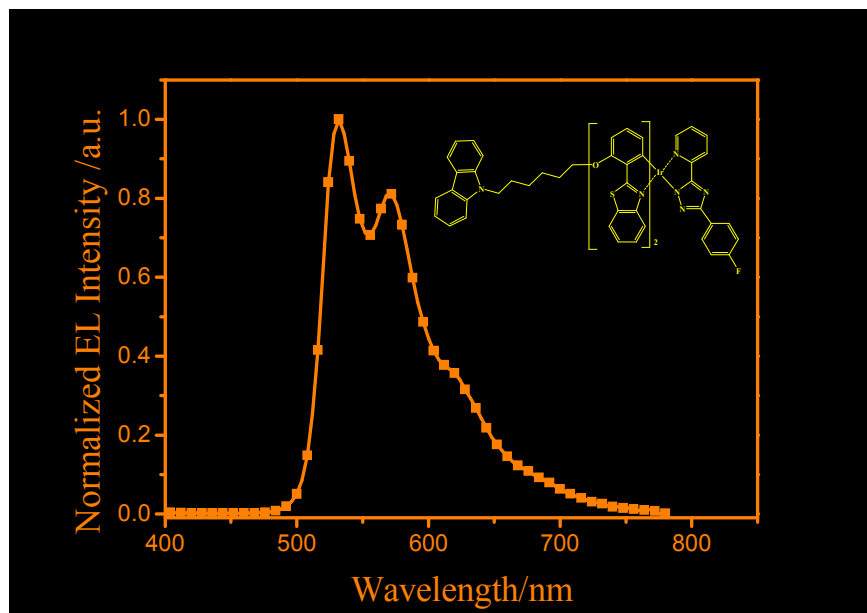
Graphical Abstract

Synthesis and photoelectric properties of a solution-processable yellow-emitting Iridium (III) complex

Yuling Wu,^{ab} Huixia Xu,^{ab} Junli Yang,^{ab} Jie Li,^{ab} Wenqing Liang,^{ab} Jing Sun,^{ab}
Hua Wang,^{ab} Bingshe Xu,^{*ab}

^a Key Laboratory of Interface Science and Engineering in Advanced Materials, Taiyuan University of Technology, Taiyuan, 030024, China.

^b Research Center of Advanced Materials Science and Technology, Taiyuan University of Technology, Taiyuan, 030024, China.



A heteroleptic iridium(III) complex [(CzhBTZ)₂Ir(fpptz)] was synthesized for efficient and stable PhOLED with spin-coating, showing a maximum brightness of 9617 cd/m², a maximum current efficiency of about 9.43 cd·A⁻¹, and International Commission on Illumination (CIE) coordinates of (0.42, 0.56), respectively.